Nonlocal response of plasmonic core–shell nanotopologies excited by dipole emitters

Mario Kupresak, Xuezhi Zheng, Raj Mittra, Guy A. E. Vandenbosch and Victor V. Moshchalkov

Electronic Supplementary Information

1. Expansion coefficients

In this section, the governing equations of the interaction between a dipole emitter and core–shell nanoparticles are provided for HW-HDM and GNOR, and Q-HDM. The analysis is performed for both metal core–dielectric shell and dielectric core–metal shell nanoparticles. The emitter is considered outside and inside the studied topologies.

1.1. Metal core–dielectric shell nanoparticle

- HW-HDM and GNOR

By following the approach in ref. 1, the fields outside and inside a metal core–dielectric shell sphere can be expanded into vector spherical harmonics as follows

$$\mathbf{E}^{DIP}(\mathbf{r}) = \begin{cases} \displaystyle\sum_{n=1}^{\infty}\sum_{m=-n}^{n}\left[d^{+}_{Hnm}h^{(1)}_{n}(k'r)\mathbf{X}^{m}_{n}(\hat{\mathbf{r}}) + \frac{i}{k'}d^{+}_{Enm}\nabla\times h^{(1)}_{n}(k'r)\mathbf{X}^{m}_{n}(\hat{\mathbf{r}})\right], & r > r' \\[4mm] \displaystyle\sum_{n=1}^{\infty}\sum_{m=-n}^{n}\left[d^{0}_{Hnm}j_{n}(k'r)\mathbf{X}^{m}_{n}(\hat{\mathbf{r}}) + \frac{i}{k'}d^{0}_{Enm}\nabla\times j_{n}(k'r)\mathbf{X}^{m}_{n}(\hat{\mathbf{r}})\right], & r < r' \end{cases} \tag{1}$$

$$\mathbf{H}^{DIP}(\mathbf{r}) = \begin{cases} \displaystyle\sqrt{\frac{\varepsilon_{0}\varepsilon'}{\mu_{0}}}\sum_{n=1}^{\infty}\sum_{m=-n}^{n}\left[d^{+}_{Enm}h^{(1)}_{n}(k'r)\mathbf{X}^{m}_{n}(\hat{\mathbf{r}}) - \frac{i}{k'}d^{+}_{Hnm}\nabla\times h^{(1)}_{n}(k'r)\mathbf{X}^{m}_{n}(\hat{\mathbf{r}})\right], & r > r' \\[4mm] \displaystyle\sqrt{\frac{\varepsilon_{0}\varepsilon'}{\mu_{0}}}\sum_{n=1}^{\infty}\sum_{m=-n}^{n}\left[d^{0}_{Enm}j_{n}(k'r)\mathbf{X}^{m}_{n}(\hat{\mathbf{r}}) - \frac{i}{k'}d^{0}_{Hnm}\nabla\times j_{n}(k'r)\mathbf{X}^{m}_{n}(\hat{\mathbf{r}})\right], & r < r' \end{cases}$$
$$\tag{2}$$

$$\mathbf{E}^{S}(\mathbf{r}) = \sum_{n=1}^{\infty}\sum_{m=-n}^{n}\left[a^{S}_{Hnm}h^{(1)}_{n}(k_{M}r)\mathbf{X}^{m}_{n}(\hat{\mathbf{r}}) + \frac{i}{k_{M}}a^{S}_{Enm}\nabla\times h^{(1)}_{n}(k_{M}r)\mathbf{X}^{m}_{n}(\hat{\mathbf{r}})\right] \tag{3}$$

$$\mathbf{H}^{S}(\mathbf{r}) = \sqrt{\frac{\varepsilon_{0}\varepsilon_{M}}{\mu_{0}}}\sum_{n=1}^{\infty}\sum_{m=-n}^{n}\left[a^{S}_{Enm}h^{(1)}_{n}(k_{M}r)\mathbf{X}^{m}_{n}(\hat{\mathbf{r}}) - \frac{i}{k_{M}}a^{S}_{Hnm}\nabla\times h^{(1)}_{n}(k_{M}r)\mathbf{X}^{m}_{n}(\hat{\mathbf{r}})\right] \tag{4}$$

$$\mathbf{E}^{T}(\mathbf{r}) = \sum_{n=1}^{\infty}\sum_{m=-n}^{n}\left[a^{T}_{Hnm}j_{n}(k_{T}r)\mathbf{X}^{m}_{n}(\hat{\mathbf{r}}) + \frac{i}{k_{T}}a^{T}_{Enm}\nabla\times j_{n}(k_{T}r)\mathbf{X}^{m}_{n}(\hat{\mathbf{r}})\right] \tag{5}$$

$$\mathbf{H}^{T}(\mathbf{r}) = \sqrt{\frac{\varepsilon_{0}\varepsilon_{T}}{\mu_{0}}}\sum_{n=1}^{\infty}\sum_{m=-n}^{n}\left[a^{T}_{Enm}j_{n}(k_{T}r)\mathbf{X}^{m}_{n}(\hat{\mathbf{r}}) - \frac{i}{k_{T}}a^{T}_{Hnm}\nabla\times j_{n}(k_{T}r)\mathbf{X}^{m}_{n}(\hat{\mathbf{r}})\right] \tag{6}$$

$$\mathbf{E}^L(\mathbf{r}) = \frac{1}{k_L} \sum_{n=1}^{\infty} \sum_{m=-n}^{n} a_{Enm}^L \nabla j_n(k_L r) Y_n^m(\hat{\mathbf{r}}) \tag{7}$$

$$\mathbf{E}^D(\mathbf{r}) = \sum_{n=1}^{\infty} \sum_{m=-n}^{n} \left[a_{Hnm}^{D,0} j_n(k_D r) \mathbf{X}_n^m(\hat{\mathbf{r}}) + \frac{i}{k_D} a_{Enm}^{D,0} \nabla \times j_n(k_D r) \mathbf{X}_n^m(\hat{\mathbf{r}}) \right.$$
$$\left. + a_{Hnm}^{D,S} y_n(k_D r) \mathbf{X}_n^m(\hat{\mathbf{r}}) + \frac{i}{k_D} a_{Enm}^{D,S} \nabla \times y_n(k_D r) \mathbf{X}_n^m(\hat{\mathbf{r}}) \right] \tag{8}$$

$$\mathbf{H}^D(\mathbf{r}) = \sqrt{\frac{\varepsilon_0 \varepsilon_D}{\mu_0}} \sum_{n=1}^{\infty} \sum_{m=-n}^{n} \left[a_{Enm}^{D,0} j_n(k_D r) \mathbf{X}_n^m(\hat{\mathbf{r}}) - \frac{i}{k_D} a_{Hnm}^{D,0} \nabla \times j_n(k_D r) \mathbf{X}_n^m(\hat{\mathbf{r}}) \right.$$
$$\left. + a_{Enm}^{D,S} y_n(k_D r) \mathbf{X}_n^m(\hat{\mathbf{r}}) - \frac{i}{k_D} a_{Hnm}^{D,S} \nabla \times y_n(k_D r) \mathbf{X}_n^m(\hat{\mathbf{r}}) \right]. \tag{9}$$

In (1)–(9), the fields generated by a dipole emitter, positioned at r', are $\mathbf{E}^{DIP}$ and $\mathbf{H}^{DIP}$; the scattered fields are $\mathbf{E}^S$ and $\mathbf{H}^S$; the transverse and longitudinal fields inside the metal core are $\mathbf{E}^T$ and $\mathbf{H}^T$, and $\mathbf{E}^L$, respectively; the fields inside the dielectric shell are $\mathbf{E}^D$ and $\mathbf{H}^D$. The vector spherical harmonics of degree n and order m are denoted by $\mathbf{X}_n^m = i/[(n(n+1))^{1/2} \sin\vartheta] \partial Y_n^m / \partial\varphi \hat{\boldsymbol{\vartheta}} - i/(n(n+1))^{1/2} \partial Y_n^m / \partial\vartheta \hat{\boldsymbol{\varphi}}$, where Y_n^m are the spherical harmonics.[2] The coefficients of $\mathbf{E}^{DIP}$ and $\mathbf{H}^{DIP}$ are defined as[1,3]

$$d_{Hnm}^+ = \frac{i(k')^3}{\varepsilon_0 \varepsilon'} \mathbf{p} \cdot j_n(k'r') \mathbf{X}_n^m(\hat{\mathbf{r}}')^* \tag{10}$$

$$d_{Hnm}^0 = \frac{i(k')^3}{\varepsilon_0 \varepsilon'} \mathbf{p} \cdot h_n^{(1)}(k'r') \mathbf{X}_n^m(\hat{\mathbf{r}}')^* \tag{11}$$

$$d_{Enm}^+ = \frac{(k')^2}{\varepsilon_0 \varepsilon'} \mathbf{p} \cdot \nabla \times j_n(k'r') \mathbf{X}_n^m(\hat{\mathbf{r}}')^* \tag{12}$$

$$d_{Enm}^0 = \frac{(k')^2}{\varepsilon_0 \varepsilon'} \mathbf{p} \cdot \nabla \times h_n^{(1)}(k'r') \mathbf{X}_n^m(\hat{\mathbf{r}}')^*. \tag{13}$$

Here, ε' and k' are the permittivity and wave number of a medium where an emitter is placed, respectively: $\varepsilon' = \varepsilon_M, k' = k_M$ for an emitter located in a surrounding medium; $\varepsilon' = \varepsilon_D, k' = k_D$ for an emitter placed inside the dielectric shell; $\mathbf{p}$ is the dipole moment, $\hat{\mathbf{r}}'$ is the source point unit vector, and the asterisk denotes the complex conjugate. The scattering coefficients are a_{Hnm}^S and a_{Enm}^S; the coefficients of the transverse and longitudinal fields inside the metal core are a_{Hnm}^T and a_{Enm}^T, and a_{Enm}^L, respectively; the coefficients of the fields inside the dielectric shell are $a_{Hnm}^{D,0}$, $a_{Hnm}^{D,S}$, and $a_{Enm}^{D,0}$, $a_{Enm}^{D,S}$. The transverse and longitudinal wave numbers are k_T and k_L, defined as[4,5]

$$k_T^2 = \varepsilon_T k_0^2, \ \varepsilon_T = \varepsilon_B - \frac{\omega_P^2}{\omega^2 + i\gamma\omega} \tag{14}$$

$$k_L^2 = \frac{1}{\eta^2}\left[\omega^2 + i\gamma\omega - \frac{\omega_P^2}{\varepsilon_B}\right] \tag{15}$$

with ε_T denoting the transverse permittivity of the metal, ε_B the permittivity of bound electrons, k_0 the vacuum wave number, ω_P the plasma frequency, and ω and γ the operating angular and damping frequencies, respectively. The nonlocal material parameter is represented by $\eta^2 = \beta^2 + D(\gamma - i\omega)$, where β stands for the hydrodynamic pressure, and D is the diffusion constant. The spherical Bessel functions of the first and second kind are represented by j_n and y_n, respectively, and the spherical Hankel function of the first kind is denoted by $h_n^{(1)}$.[6]

In order to compute the scattering coefficients and the coefficients of the fields inside the nanoparticle, one requires applying the classical boundary conditions, which are supplemented by the Sauter ABC.[7] First, by placing an emitter outside the structure-under-study, the boundary conditions read

$$E_\vartheta^{DIP}\Big|_{r=R_2} + E_\vartheta^{S}\Big|_{r=R_2} = E_\vartheta^{D}\Big|_{r=R_2} \tag{16}$$

$$E_\varphi^{DIP}\Big|_{r=R_2} + E_\varphi^{S}\Big|_{r=R_2} = E_\varphi^{D}\Big|_{r=R_2} \tag{17}$$

$$H_\vartheta^{DIP}\Big|_{r=R_2} + H_\vartheta^{S}\Big|_{r=R_2} = H_\vartheta^{D}\Big|_{r=R_2} \tag{18}$$

$$H_\varphi^{DIP}\Big|_{r=R_2} + H_\varphi^{S}\Big|_{r=R_2} = H_\varphi^{D}\Big|_{r=R_2} \tag{19}$$

$$E_\vartheta^{D}\Big|_{r=R_1} = E_\vartheta^{T}\Big|_{r=R_1} + E_\vartheta^{L}\Big|_{r=R_1} \tag{20}$$

$$E_\varphi^{D}\Big|_{r=R_1} = E_\varphi^{T}\Big|_{r=R_1} + E_\varphi^{L}\Big|_{r=R_1} \tag{21}$$

$$H_\vartheta^{D}\Big|_{r=R_1} = H_\vartheta^{T}\Big|_{r=R_1} \tag{22}$$

$$H_\varphi^{D}\Big|_{r=R_1} = H_\varphi^{T}\Big|_{r=R_1} \tag{23}$$

$$J_r\Big|_{r=R_1} = 0. \tag{24}$$

By expressing the hydrodynamic current $\mathbf{J}$ in (24) in terms of the electric field,[4] and employing the corresponding expansions (1)–(9), together with the relations

$$\nabla \times g_n(kr)\mathbf{X}_n^m = \frac{i\sqrt{n(n+1)}g_n(kr)}{r}Y_n^m\hat{\mathbf{r}} + \frac{i[krg_n(kr)]'}{r\sqrt{n(n+1)}}\frac{\partial Y_n^m}{\partial\vartheta}\hat{\boldsymbol{\vartheta}}$$
$$+ \frac{i[krg_n(kr)]'}{\sin\vartheta\sqrt{n(n+1)}}\frac{\partial Y_n^m}{\partial\varphi}\hat{\boldsymbol{\varphi}} \tag{25}$$

$$\nabla g_n(kr)Y_n^m = k g_n'(kr)Y_n^m \hat{\mathbf{r}} + \frac{g_n(kr)}{r}\frac{\partial Y_n^m}{\partial \vartheta}\hat{\boldsymbol{\vartheta}} + \frac{g_n(kr)}{r\sin\vartheta}\frac{\partial Y_n^m}{\partial \varphi}\hat{\boldsymbol{\varphi}} \qquad (26)$$

where $g_n = j_n, y_n, h_n^{(1)}$ and the primes denote differentiation with respect to the argument of the radial functions, the following set of equations is obtained

$$j_n(k_M R_2)d_{Hnm}^0 + h_n^{(1)}(k_M R_2)a_{Hnm}^S = j_n(k_D R_2)a_{Hnm}^{D,0} + y_n(k_D R_2)a_{Hnm}^{D,S} \qquad (27)$$

$$k_D[k_M R_2 j_n(k_M R_2)]' d_{Enm}^0 + k_D[k_M R_2 h_n^{(1)}(k_M R_2)]' a_{Enm}^S =$$
$$k_M[k_D R_2 j_n(k_D R_2)]' a_{Enm}^{D,0} + k_M[k_D R_2 y_n(k_D R_2)]' a_{Enm}^{D,S} \qquad (28)$$

$$k_M j_n(k_M R_2)d_{Enm}^0 + k_M h_n^{(1)}(k_M R_2)a_{Enm}^S = k_D j_n(k_D R_2)a_{Enm}^{D,0} + k_D y_n(k_D R_2)a_{Enm}^{D,S} \qquad (29)$$

$$[k_M R_2 j_n(k_M R_2)]' d_{Hnm}^0 + [k_M R_2 h_n^{(1)}(k_M R_2)]' a_{Hnm}^S = [k_D R_2 j_n(k_D R_2)]' a_{Hnm}^{D,0}$$
$$+[k_D R_2 y_n(k_D R_2)]' a_{Hnm}^{D,S} \qquad (30)$$

$$j_n(k_D R_1)a_{Hnm}^{D,0} + y_n(k_D R_1)a_{Hnm}^{D,S} = j_n(k_T R_1)a_{Hnm}^T \qquad (31)$$

$$-k_T k_L[k_D R_1 j_n(k_D R_1)]' a_{Enm}^{D,0} - k_T k_L[k_D R_1 y_n(k_D R_1)]' a_{Enm}^{D,S} =$$
$$-k_D k_L[k_T R_1 j_n(k_T R_1)]' a_{Enm}^T + k_D k_T \sqrt{n(n+1)}j_n(k_L R_1)a_{Enm}^L \qquad (32)$$

$$k_D j_n(k_D R_1)a_{Enm}^{D,0} + k_D y_n(k_D R_1)a_{Enm}^{D,S} = k_T j_n(k_T R_1)a_{Enm}^T \qquad (33)$$

$$[k_D R_1 j_n(k_D R_1)]' a_{Hnm}^{D,0} + [k_D R_1 y_n(k_D R_1)]' a_{Hnm}^{D,S} = [k_T R_1 j_n(k_T R_1)]' a_{Hnm}^T \qquad (34)$$

$$-(\varepsilon_T - \varepsilon_B)\sqrt{n(n+1)}j_n(k_T R_1)a_{Enm}^T = \varepsilon_B k_T R_1 j_n'(k_L R_1)a_{Enm}^L. \qquad (35)$$

When an emitter is located inside the dielectric shell, the classical boundary conditions are the following

$$E_\vartheta^S\Big|_{r=R_2} = E_\vartheta^{DIP}\Big|_{r=R_2} + E_\vartheta^D\Big|_{r=R_2} \qquad (36)$$

$$E_\varphi^S\Big|_{r=R_2} = E_\varphi^{DIP}\Big|_{r=R_2} + E_\varphi^D\Big|_{r=R_2} \qquad (37)$$

$$H_\vartheta^S\Big|_{r=R_2} = H_\vartheta^{DIP}\Big|_{r=R_2} + H_\vartheta^D\Big|_{r=R_2} \qquad (38)$$

$$H_\varphi^S\Big|_{r=R_2} = H_\varphi^{DIP}\Big|_{r=R_2} + H_\varphi^D\Big|_{r=R_2} \qquad (39)$$

$$E_\vartheta^{DIP}\Big|_{r=R_1} + E_\vartheta^D\Big|_{r=R_1} = E_\vartheta^T\Big|_{r=R_1} + E_\vartheta^L\Big|_{r=R_1} \qquad (40)$$

$$E_{\varphi}^{DIP}\Big|_{r=R_1} + E_{\varphi}^{D}\Big|_{r=R_1} = E_{\varphi}^{T}\Big|_{r=R_1} + E_{\varphi}^{L}\Big|_{r=R_1} \tag{41}$$

$$H_{\vartheta}^{DIP}\Big|_{r=R_1} + H_{\vartheta}^{D}\Big|_{r=R_1} = H_{\vartheta}^{T}\Big|_{r=R_1} \tag{42}$$

$$H_{\varphi}^{DIP}\Big|_{r=R_1} + H_{\varphi}^{D}\Big|_{r=R_1} = H_{\varphi}^{T}\Big|_{r=R_1}. \tag{43}$$

The expansion of (36)–(43), using (1)–(9), (25), and (26), yields

$$h_n^{(1)}(k_M R_2)a_{Hnm}^S = h_n^{(1)}(k_D R_2)d_{Hnm}^+ + j_n(k_D R_2)a_{Hnm}^{D,0} + y_n(k_D R_2)a_{Hnm}^{D,S} \tag{44}$$

$$k_D[k_M R_2 h_n^{(1)}(k_M R_2)]' a_{Enm}^S = k_M[k_D R_2 h_n^{(1)}(k_D R_2)]' d_{Enm}^+$$
$$+k_M[k_D R_2 j_n(k_D R_2)]' a_{Enm}^{D,0} + k_M[k_D R_2 y_n(k_D R_2)]' a_{Enm}^{D,S} \tag{45}$$

$$k_M h_n^{(1)}(k_M R_2)a_{Enm}^S = k_D h_n^{(1)}(k_D R_2)d_{Enm}^+ + k_D j_n(k_D R_2)a_{Enm}^{D,0} + k_D y_n(k_D R_2)a_{Enm}^{D,S} \tag{46}$$

$$[k_M R_2 h_n^{(1)}(k_M R_2)]' a_{Hnm}^S = [k_D R_2 h_n^{(1)}(k_D R_2)]' d_{Hnm}^+ + [k_D R_2 j_n(k_D R_2)]' a_{Hnm}^{D,0}$$
$$+[k_D R_2 y_n(k_D R_2)]' a_{Hnm}^{D,S} \tag{47}$$

$$j_n(k_D R_1)d_{Hnm}^0 + j_n(k_D R_1)a_{Hnm}^{D,0} + y_n(k_D R_1)a_{Hnm}^{D,S} = j_n(k_T R_1)a_{Hnm}^T \tag{48}$$

$$-k_T k_L[k_D R_1 j_n(k_D R_1)]' d_{Enm}^0 - k_T k_L[k_D R_1 j_n(k_D R_1)]' a_{Enm}^{D,0}$$
$$-k_T k_L[k_D R_1 y_n(k_D R_1)]' a_{Enm}^{D,S} = -k_D k_L[k_T R_1 j_n(k_T R_1)]' a_{Enm}^T$$
$$+k_D k_T \sqrt{n(n+1)} j_n(k_L R_1)a_{Enm}^L \tag{49}$$

$$k_D j_n(k_D R_1)d_{Enm}^0 + k_D j_n(k_D R_1)a_{Enm}^{D,0} + k_D y_n(k_D R_1)a_{Enm}^{D,S} = k_T j_n(k_T R_1)a_{Enm}^T \tag{50}$$

$$[k_D R_1 j_n(k_D R_1)]' d_{Hnm}^0 + [k_D R_1 j_n(k_D R_1)]' a_{Hnm}^{D,0} + [k_D R_1 y_n(k_D R_1)]' a_{Hnm}^{D,S} =$$
$$[k_T R_1 j_n(k_T R_1)]' a_{Hnm}^T. \tag{51}$$

The abovementioned set of equations needs to be supplemented by the ABC in (35), in order to calculate the associated coefficients.

- Q-HDM

Within the framework of Q-HDM, the longitudinal fields inside the metal core are defined as

$$\mathbf{E}^{L1}(\mathbf{r}) = \frac{1}{k_{L1}} \sum_{n=1}^{\infty} \sum_{m=-n}^{n} a_{Enm}^{L1} \nabla j_n(k_{L1}r)Y_n^m(\hat{\mathbf{r}}) \tag{52}$$

$$\mathbf{E}^{L2}(\mathbf{r}) = \frac{1}{k_{L2}} \sum_{n=1}^{\infty} \sum_{m=-n}^{n} a_{Enm}^{L2} \nabla j_n(k_{L2}r) Y_n^m(\hat{\mathbf{r}}). \tag{53}$$

In (52) and (53), the longitudinal wave numbers k_{L1} and k_{L2} are given as

$$k_{L1,2}^2 = \frac{-\beta^2}{2\alpha^2} \pm \frac{\beta^2}{2\alpha^2}\left[1 + \frac{4\alpha^2}{\beta^4}(\omega^2 + i\gamma\omega - \frac{\omega_P^2}{\varepsilon_B})\right]^{1/2} \tag{54}$$

with α taking the contribution of quantum diffraction effects into account.[8] The associated coefficients may be calculated by imposing the classical boundary conditions that are augmented by the corresponding ABCs. Considering an emitter outside the nanoparticle, compared with HW-HDM, (27)–(31), (33), and (34) are identical, while the remaining two equations are the following

$$\begin{aligned}
&-k_T k_{L1} k_{L2} [k_D R_1 j_n(k_D R_1)]' a_{Enm}^{D,0} - k_T k_{L1} k_{L2} [k_D R_1 y_n(k_D R_1)]' a_{Enm}^{D,S} = \\
&-k_D k_{L1} k_{L2} [k_T R_1 j_n(k_T R_1)]' a_{Enm}^{T} + k_D k_T k_{L2} \sqrt{n(n+1)} j_n(k_{L1} R_1) a_{Enm}^{L1} \\
&+k_D k_T k_{L1} \sqrt{n(n+1)} j_n(k_{L2} R_1) a_{Enm}^{L2}
\end{aligned} \tag{55}$$

$$\begin{aligned}
&-(\varepsilon_T - \varepsilon_B)\sqrt{n(n+1)} j_n(k_T R_1) a_{Enm}^{T} = \varepsilon_B k_T R_1 j_n'(k_{L1} R_1) a_{Enm}^{L1} \\
&+\varepsilon_B k_T R_1 j_n'(k_{L2} R_1) a_{Enm}^{L2}.
\end{aligned} \tag{56}$$

On top, the application of the ABC $\nabla^2 n = 0$ yields[8]

$$k_{L1}^3 j_n(k_{L1} R_1) a_{Enm}^{L1} = -k_{L2}^3 j_n(k_{L2} R_1) a_{Enm}^{L2}. \tag{57}$$

Similarly, in the case of an emitter located inside the dielectric shell, (44)–(48), (50), (51), together with (55), (56), are identical, and the remaining equation to be treated is

$$\begin{aligned}
&-k_T k_{L1} k_{L2} [k_D R_1 j_n(k_D R_1)]' d_{Enm}^{0} - k_T k_{L1} k_{L2} [k_D R_1 j_n(k_D R_1)]' a_{Enm}^{D,0} \\
&-k_T k_{L1} k_{L2} [k_D R_1 y_n(k_D R_1)]' a_{Enm}^{D,S} = -k_D k_{L1} k_{L2} [k_T R_1 j_n(k_T R_1)]' a_{Enm}^{T} \\
&+k_D k_T k_{L2} \sqrt{n(n+1)} j_n(k_{L1} R_1) a_{Enm}^{L1} + k_D k_T k_{L1} \sqrt{n(n+1)} j_n(k_{L2} R_1) a_{Enm}^{L2}.
\end{aligned} \tag{58}$$

1.2. Dielectric core–metal shell nanoparticle

- HW-HDM and GNOR

Compared with the metal core–dielectric shell structure, the fields inside the other studied topology (viz., the dielectric core–metal shell) are the following[1]

$$\mathbf{E}^T(\mathbf{r}) = \sum_{n=1}^{\infty} \sum_{m=-n}^{n} \left[a_{Hnm}^{T,0} j_n(k_T r) \mathbf{X}_n^m(\hat{\mathbf{r}}) + \frac{i}{k_T} a_{Enm}^{T,0} \nabla \times j_n(k_T r) \mathbf{X}_n^m(\hat{\mathbf{r}}) \right. $$
$$\left. + a_{Hnm}^{T,S} y_n(k_T r) \mathbf{X}_n^m(\hat{\mathbf{r}}) + \frac{i}{k_T} a_{Enm}^{T,S} \nabla \times y_n(k_T r) \mathbf{X}_n^m(\hat{\mathbf{r}}) \right] \tag{59}$$

$$\mathbf{H}^T(\mathbf{r}) = \sqrt{\frac{\varepsilon_0 \varepsilon_T}{\mu_0}} \sum_{n=1}^{\infty} \sum_{m=-n}^{n} \left[a_{Enm}^{T,0} j_n(k_T r) \mathbf{X}_n^m(\hat{\mathbf{r}}) - \frac{i}{k_T} a_{Hnm}^{T,0} \nabla \times j_n(k_T r) \mathbf{X}_n^m(\hat{\mathbf{r}}) \right. $$
$$\left. + a_{Enm}^{T,S} y_n(k_T r) \mathbf{X}_n^m(\hat{\mathbf{r}}) - \frac{i}{k_T} a_{Hnm}^{T,S} \nabla \times y_n(k_T r) \mathbf{X}_n^m(\hat{\mathbf{r}}) \right] \tag{60}$$

$$\mathbf{E}^L(\mathbf{r}) = \frac{1}{k_L} \sum_{n=1}^{\infty} \sum_{m=-n}^{n} \left[a_{Enm}^{L,0} \nabla j_n(k_L r) Y_n^m(\hat{\mathbf{r}}) + a_{Enm}^{L,S} \nabla y_n(k_L r) Y_n^m(\hat{\mathbf{r}}) \right] \tag{61}$$

$$\mathbf{E}^D(\mathbf{r}) = \sum_{n=1}^{\infty} \sum_{m=-n}^{n} \left[a_{Hnm}^{D} j_n(k_D r) \mathbf{X}_n^m(\hat{\mathbf{r}}) + \frac{i}{k_D} a_{Enm}^{D} \nabla \times j_n(k_D r) \mathbf{X}_n^m(\hat{\mathbf{r}}) \right] \tag{62}$$

$$\mathbf{H}^D(\mathbf{r}) = \sqrt{\frac{\varepsilon_0 \varepsilon_D}{\mu_0}} \sum_{n=1}^{\infty} \sum_{m=-n}^{n} \left[a_{Enm}^{D} j_n(k_D r) \mathbf{X}_n^m(\hat{\mathbf{r}}) - \frac{i}{k_D} a_{Hnm}^{D} \nabla \times j_n(k_D r) \mathbf{X}_n^m(\hat{\mathbf{r}}) \right]. \tag{63}$$

In (59)–(63), $\mathbf{E}^T$, $\mathbf{H}^T$, and $\mathbf{E}^L$ denote the transverse and longitudinal fields inside the metal shell, and $\mathbf{E}^D$ and $\mathbf{H}^D$ are the fields inside the dielectric core, with the corresponding coefficients. Considering an emitter outside the nanoparticle, the boundary conditions read

$$E_\vartheta^{DIP}\Big|_{r=R_2} + E_\vartheta^{S}\Big|_{r=R_2} = E_\vartheta^{T}\Big|_{r=R_2} + E_\vartheta^{L}\Big|_{r=R_2} \tag{64}$$

$$E_\varphi^{DIP}\Big|_{r=R_2} + E_\varphi^{S}\Big|_{r=R_2} = E_\varphi^{T}\Big|_{r=R_2} + E_\varphi^{L}\Big|_{r=R_2} \tag{65}$$

$$H_\vartheta^{DIP}\Big|_{r=R_2} + H_\vartheta^{S}\Big|_{r=R_2} = H_\vartheta^{T}\Big|_{r=R_2} \tag{66}$$

$$H_\varphi^{DIP}\Big|_{r=R_2} + H_\varphi^{S}\Big|_{r=R_2} = H_\varphi^{T}\Big|_{r=R_2} \tag{67}$$

$$J_r\Big|_{r=R_2} = 0 \tag{68}$$

$$E_\vartheta^{T}\Big|_{r=R_1} + E_\vartheta^{L}\Big|_{r=R_1} = E_\vartheta^{D}\Big|_{r=R_1} \tag{69}$$

$$E_\varphi^{T}\Big|_{r=R_1} + E_\varphi^{L}\Big|_{r=R_1} = E_\varphi^{D}\Big|_{r=R_1} \tag{70}$$

$$H_\vartheta^{T}\Big|_{r=R_1} = H_\vartheta^{D}\Big|_{r=R_1} \tag{71}$$

$$H_\varphi^{T}\Big|_{r=R_1} = H_\varphi^{D}\Big|_{r=R_1} \tag{72}$$

$$J_r\big|_{r=R_1} = 0. \tag{73}$$

The expansion of (64)–(73) yields the following set of equations

$$j_n(k_M R_2)d^0_{Hnm} + h_n^{(1)}(k_M R_2)a^S_{Hnm} = j_n(k_T R_2)a^{T,0}_{Hnm} + y_n(k_T R_2)a^{T,S}_{Hnm} \tag{74}$$

$$\begin{aligned}
&-k_T k_L [k_M R_2 j_n(k_M R_2)]' d^0_{Enm} - k_T k_L [k_M R_2 h_n^{(1)}(k_M R_2)]' a^S_{Enm} = \\
&-k_M k_L [k_T R_2 j_n(k_T R_2)]' a^{T,0}_{Enm} - k_M k_L [k_T R_2 y_n(k_T R_2)]' a^{T,S}_{Enm} \\
&+k_T k_M \sqrt{n(n+1)} j_n(k_L R_2)a^{L,0}_{Enm} + k_T k_M \sqrt{n(n+1)} y_n(k_L R_2)a^{L,S}_{Enm}
\end{aligned} \tag{75}$$

$$k_M j_n(k_M R_2)d^0_{Enm} + k_M h_n^{(1)}(k_M R_2)a^S_{Enm} = k_T j_n(k_T R_2)a^{T,0}_{Enm} + k_T y_n(k_T R_2)a^{T,S}_{Enm} \tag{76}$$

$$\begin{aligned}
&[k_M R_2 j_n(k_M R_2)]' d^0_{Hnm} + [k_M R_2 h_n^{(1)}(k_M R_2)]' a^S_{Hnm} = [k_T R_2 j_n(k_T R_2)]' a^{T,0}_{Hnm} \\
&+[k_T R_2 y_n(k_T R_2)]' a^{T,S}_{Hnm}
\end{aligned} \tag{77}$$

$$\begin{aligned}
&-(\varepsilon_T - \varepsilon_B)\sqrt{n(n+1)} j_n(k_T R_2)a^{T,0}_{Enm} - (\varepsilon_T - \varepsilon_B)\sqrt{n(n+1)} y_n(k_T R_2)a^{T,S}_{Enm} = \\
&\varepsilon_B k_T R_2 j_n'(k_L R_2)a^{L,0}_{Enm} + \varepsilon_B k_T R_2 y_n'(k_L R_2)a^{L,S}_{Enm}
\end{aligned} \tag{78}$$

$$j_n(k_T R_1)a^{T,0}_{Hnm} + y_n(k_T R_1)a^{T,S}_{Hnm} = j_n(k_D R_1)a^D_{Hnm} \tag{79}$$

$$\begin{aligned}
&-k_D k_L [k_T R_1 j_n(k_T R_1)]' a^{T,0}_{Enm} - k_D k_L [k_T R_1 y_n(k_T R_1)]' a^{T,S}_{Enm} \\
&+k_D k_T \sqrt{n(n+1)} j_n(k_L R_1)a^{L,0}_{Enm} + k_D k_T \sqrt{n(n+1)} y_n(k_L R_1)a^{L,S}_{Enm} = \\
&-k_T k_L [k_D R_1 j_n(k_D R_1)]' a^D_{Enm}
\end{aligned} \tag{80}$$

$$k_T j_n(k_T R_1)a^{T,0}_{Enm} + k_T y_n(k_T R_1)a^{T,S}_{Enm} = k_D j_n(k_D R_1)a^D_{Enm} \tag{81}$$

$$[k_T R_1 j_n(k_T R_1)]' a^{T,0}_{Hnm} + [k_T R_1 y_n(k_T R_1)]' a^{T,S}_{Hnm} = [k_D R_1 j_n(k_D R_1)]' a^D_{Hnm} \tag{82}$$

$$\begin{aligned}
&-(\varepsilon_T - \varepsilon_B)\sqrt{n(n+1)} j_n(k_T R_1)a^{T,0}_{Enm} - (\varepsilon_T - \varepsilon_B)\sqrt{n(n+1)} y_n(k_T R_1)a^{T,S}_{Enm} = \\
&\varepsilon_B k_T R_1 j_n'(k_L R_1)a^{L,0}_{Enm} + \varepsilon_B k_T R_1 y_n'(k_L R_1)a^{L,S}_{Enm}.
\end{aligned} \tag{83}$$

When an emitter is located inside the dielectric core, the following classical boundary conditions hold

$$E^S_\vartheta\big|_{r=R_2} = E^T_\vartheta\big|_{r=R_2} + E^L_\vartheta\big|_{r=R_2} \tag{84}$$

$$E^S_\varphi\big|_{r=R_2} = E^T_\varphi\big|_{r=R_2} + E^L_\varphi\big|_{r=R_2} \tag{85}$$

$$H_\vartheta^S\Big|_{r=R_2} = H_\vartheta^T\Big|_{r=R_2} \tag{86}$$

$$H_\varphi^S\Big|_{r=R_2} = H_\varphi^T\Big|_{r=R_2} \tag{87}$$

$$E_\vartheta^T\Big|_{r=R_1} + E_\vartheta^L\Big|_{r=R_1} = E_\vartheta^{DIP}\Big|_{r=R_1} + E_\vartheta^D\Big|_{r=R_1} \tag{88}$$

$$E_\varphi^T\Big|_{r=R_1} + E_\varphi^L\Big|_{r=R_1} = E_\varphi^{DIP}\Big|_{r=R_1} + E_\varphi^D\Big|_{r=R_1} \tag{89}$$

$$H_\vartheta^T\Big|_{r=R_1} = H_\vartheta^{DIP}\Big|_{r=R_1} + H_\vartheta^D\Big|_{r=R_1} \tag{90}$$

$$H_\varphi^T\Big|_{r=R_1} = H_\varphi^{DIP}\Big|_{r=R_1} + H_\varphi^D\Big|_{r=R_1}. \tag{91}$$

By expanding (84)–(91), the following set of equations is obtained

$$h_n^{(1)}(k_M R_2)a_{Hnm}^S = j_n(k_T R_2)a_{Hnm}^{T,0} + y_n(k_T R_2)a_{Hnm}^{T,S} \tag{92}$$

$$-k_T k_L [k_M R_2 h_n^{(1)}(k_M R_2)]' a_{Enm}^S = -k_M k_L [k_T R_2 j_n(k_T R_2)]' a_{Enm}^{T,0}$$
$$-k_M k_L [k_T R_2 y_n(k_T R_2)]' a_{Enm}^{T,S} + k_T k_M \sqrt{n(n+1)} j_n(k_L R_2)a_{Enm}^{L,0}$$
$$+k_T k_M \sqrt{n(n+1)} y_n(k_L R_2)a_{Enm}^{L,S} \tag{93}$$

$$k_M h_n^{(1)}(k_M R_2)a_{Enm}^S = k_T j_n(k_T R_2)a_{Enm}^{T,0} + k_T y_n(k_T R_2)a_{Enm}^{T,S} \tag{94}$$

$$[k_M R_2 h_n^{(1)}(k_M R_2)]' a_{Hnm}^S = [k_T R_2 j_n(k_T R_2)]' a_{Hnm}^{T,0} + [k_T R_2 y_n(k_T R_2)]' a_{Hnm}^{T,S} \tag{95}$$

$$j_n(k_T R_1)a_{Hnm}^{T,0} + y_n(k_T R_1)a_{Hnm}^{T,S} = h_n^{(1)}(k_D R_1)d_{Hnm}^+ + j_n(k_D R_1)a_{Hnm}^D \tag{96}$$

$$-k_D k_L [k_T R_1 j_n(k_T R_1)]' a_{Enm}^{T,0} - k_D k_L [k_T R_1 y_n(k_T R_1)]' a_{Enm}^{T,S}$$
$$+k_D k_T \sqrt{n(n+1)} j_n(k_L R_1)a_{Enm}^{L,0} + k_D k_T \sqrt{n(n+1)} y_n(k_L R_1)a_{Enm}^{L,S} =$$
$$-k_T k_L [k_D R_1 h_n^{(1)}(k_D R_1)]' d_{Enm}^+ - k_T k_L [k_D R_1 j_n(k_D R_1)]' a_{Enm}^D \tag{97}$$

$$k_T j_n(k_T R_1)a_{Enm}^{T,0} + k_T y_n(k_T R_1)a_{Enm}^{T,S} = k_D h_n^{(1)}(k_D R_1)d_{Enm}^+ + k_D j_n(k_D R_1)a_{Enm}^D \tag{98}$$

$$[k_T R_1 j_n(k_T R_1)]' a_{Hnm}^{T,0} + [k_T R_1 y_n(k_T R_1)]' a_{Hnm}^{T,S} = [k_D R_1 h_n^{(1)}(k_D R_1)]' d_{Hnm}^+$$
$$+[k_D R_1 j_n(k_D R_1)]' a_{Hnm}^D. \tag{99}$$

The associated coefficients are generated by solving (92)–(99), together with the corresponding ABCs in (78) and (83).

- Q-HDM

The longitudinal fields inside the metal shell are expressed as

$$\mathbf{E}^{L1}(\mathbf{r}) = \frac{1}{k_{L1}} \sum_{n=1}^{\infty} \sum_{m=-n}^{n} \left[a_{Enm}^{L1,0} \nabla j_n(k_{L1}r) Y_n^m(\hat{\mathbf{r}}) + a_{Enm}^{L1,S} \nabla y_n(k_{L1}r) Y_n^m(\hat{\mathbf{r}}) \right] \quad (100)$$

$$\mathbf{E}^{L2}(\mathbf{r}) = \frac{1}{k_{L2}} \sum_{n=1}^{\infty} \sum_{m=-n}^{n} \left[a_{Enm}^{L2,0} \nabla j_n(k_{L2}r) Y_n^m(\hat{\mathbf{r}}) + a_{Enm}^{L2,S} \nabla y_n(k_{L2}r) Y_n^m(\hat{\mathbf{r}}) \right]. \quad (101)$$

Considering the emitter outside the structure-under-study, compared with HW-HDM, (74), (76), (77), (79), (81), and (82) are identical, while the other four equations read

$$-k_T k_{L1} k_{L2} [k_M R_2 j_n(k_M R_2)]' d_{Enm}^0 - k_T k_{L1} k_{L2} [k_M R_2 h_n^{(1)}(k_M R_2)]' a_{Enm}^S =$$
$$-k_M k_{L1} k_{L2} [k_T R_2 j_n(k_T R_2)]' a_{Enm}^{T,0} - k_M k_{L1} k_{L2} [k_T R_2 y_n(k_T R_2)]' a_{Enm}^{T,S}$$
$$+k_T k_M k_{L2} \sqrt{n(n+1)} j_n(k_{L1} R_2) a_{Enm}^{L1,0} + k_T k_M k_{L2} \sqrt{n(n+1)} y_n(k_{L1} R_2) a_{Enm}^{L1,S}$$
$$+k_T k_M k_{L1} \sqrt{n(n+1)} j_n(k_{L2} R_2) a_{Enm}^{L2,0} + k_T k_M k_{L1} \sqrt{n(n+1)} y_n(k_{L2} R_2) a_{Enm}^{L2,S} \quad (102)$$

$$-(\varepsilon_T - \varepsilon_B) \sqrt{n(n+1)} j_n(k_T R_2) a_{Enm}^{T,0} - (\varepsilon_T - \varepsilon_B) \sqrt{n(n+1)} y_n(k_T R_2) a_{Enm}^{T,S} =$$
$$\varepsilon_B k_T R_2 j_n'(k_{L1} R_2) a_{Enm}^{L1,0} + \varepsilon_B k_T R_2 y_n'(k_{L1} R_2) a_{Enm}^{L1,S}$$
$$+\varepsilon_B k_T R_2 j_n'(k_{L2} R_2) a_{Enm}^{L2,0} + \varepsilon_B k_T R_2 y_n'(k_{L2} R_2) a_{Enm}^{L2,S} \quad (103)$$

$$-k_D k_{L1} k_{L2} [k_T R_1 j_n(k_T R_1)]' a_{Enm}^{T,0} - k_D k_{L1} k_{L2} [k_T R_1 y_n(k_T R_1)]' a_{Enm}^{T,S}$$
$$+k_D k_T k_{L2} \sqrt{n(n+1)} j_n(k_{L1} R_1) a_{Enm}^{L1,0} + k_D k_T k_{L2} \sqrt{n(n+1)} y_n(k_{L1} R_1) a_{Enm}^{L1,S}$$
$$+k_D k_T k_{L1} \sqrt{n(n+1)} j_n(k_{L2} R_1) a_{Enm}^{L2,0} + k_D k_T k_{L1} \sqrt{n(n+1)} y_n(k_{L2} R_1) a_{Enm}^{L2,S} =$$
$$-k_T k_{L1} k_{L2} [k_D R_1 j_n(k_D R_1)]' a_{Enm}^D \quad (104)$$

$$-(\varepsilon_T - \varepsilon_B) \sqrt{n(n+1)} j_n(k_T R_1) a_{Enm}^{T,0} - (\varepsilon_T - \varepsilon_B) \sqrt{n(n+1)} y_n(k_T R_1) a_{Enm}^{T,S} =$$
$$\varepsilon_B k_T R_1 j_n'(k_{L1} R_1) a_{Enm}^{L1,0} + \varepsilon_B k_T R_1 y_n'(k_{L1} R_1) a_{Enm}^{L1,S}$$
$$+\varepsilon_B k_T R_1 j_n'(k_{L2} R_1) a_{Enm}^{L2,0} + \varepsilon_B k_T R_1 y_n'(k_{L2} R_1) a_{Enm}^{L2,S}. \quad (105)$$

On top, the application of the ABC $\nabla^2 n = 0$ yields

$$k_{L1}^3 j_n(k_{L1} R_2) a_{Enm}^{L1,0} + k_{L1}^3 y_n(k_{L1} R_2) a_{Enm}^{L1,S} = -k_{L2}^3 j_n(k_{L2} R_2) a_{Enm}^{L2,0}$$
$$-k_{L2}^3 y_n(k_{L2} R_2) a_{Enm}^{L2,S} \quad (106)$$

$$k_{L1}^3 j_n(k_{L1} R_1) a_{Enm}^{L1,0} + k_{L1}^3 y_n(k_{L1} R_1) a_{Enm}^{L1,S} = -k_{L2}^3 j_n(k_{L2} R_1) a_{Enm}^{L2,0}$$
$$-k_{L2}^3 y_n(k_{L2} R_1) a_{Enm}^{L2,S}. \quad (107)$$

As for an emitter located inside the core, (92), (94)–(96), (98), (99), (103), (105)–(107) remain the same, and the other two equations to be treated are

$$
\begin{aligned}
&-k_M k_{L1} k_{L2} [k_T R_2 j_n(k_T R_2)]' a_{Enm}^{T,0} - k_M k_{L1} k_{L2} [k_T R_2 y_n(k_T R_2)]' a_{Enm}^{T,S} \\
&+k_M k_T k_{L2} \sqrt{n(n+1)} j_n(k_{L1} R_2) a_{Enm}^{L1,0} + k_M k_T k_{L2} \sqrt{n(n+1)} y_n(k_{L1} R_2) a_{Enm}^{L1,S} \\
&+k_M k_T k_{L1} \sqrt{n(n+1)} j_n(k_{L2} R_2) a_{Enm}^{L2,0} + k_M k_T k_{L1} \sqrt{n(n+1)} y_n(k_{L2} R_2) a_{Enm}^{L2,S} = \\
&-k_T k_{L1} k_{L2} [k_M R_2 h_n^{(1)}(k_M R_2)]' a_{Enm}^{S}
\end{aligned}
\tag{108}
$$

$$
\begin{aligned}
&-k_T k_{L1} k_{L2} [k_D R_1 h_n^{(1)}(k_D R_1)]' d_{Enm}^{+} - k_T k_{L1} k_{L2} [k_D R_1 j_n(k_D R_1)]' a_{Enm}^{D} = \\
&-k_D k_{L1} k_{L2} [k_T R_1 j_n(k_T R_1)]' a_{Enm}^{T,0} - k_D k_{L1} k_{L2} [k_T R_1 y_n(k_T R_1)]' a_{Enm}^{T,S} \\
&+k_D k_T k_{L2} \sqrt{n(n+1)} j_n(k_{L1} R_1) a_{Enm}^{L1,0} + k_D k_T k_{L2} \sqrt{n(n+1)} y_n(k_{L1} R_1) a_{Enm}^{L1,S} \\
&+k_D k_T k_{L1} \sqrt{n(n+1)} j_n(k_{L2} R_1) a_{Enm}^{L2,0} + k_D k_T k_{L1} \sqrt{n(n+1)} y_n(k_{L2} R_1) a_{Enm}^{L2,S}.
\end{aligned}
\tag{109}
$$

2. Observed features

The normalized total decay rate of the emitter–nanoparticle system $\Gamma/\Gamma_0 = \Gamma_{rad}/\Gamma_0 + \Gamma_{nrad}/\Gamma_0$, with Γ_{rad}/Γ_0 and Γ_{nrad}/Γ_0 being the normalized radiative and nonradiative decay rates, may be expressed as[9]

$$
\frac{\Gamma}{\Gamma_0} = \frac{P}{P_0} = \frac{6\pi\sqrt{\varepsilon'}}{k'} \hat{\mathbf{p}} \cdot \mathrm{Im}\left\{ \overset{\leftrightarrow}{\mathbf{G}}(\mathbf{r}',\mathbf{r}') \right\} \cdot \hat{\mathbf{p}}.
\tag{110}
$$

In (110), $P = P_{rad} + P_{nrad}$ stands for the total power of the system, $P_0 = c k_0^4 p^2/(12\pi\varepsilon_0)$ is the radiated power of an isolated emitter in vacuum, ε' and k' denote the permittivity and wave number of a medium where an emitter is located, respectively, as discussed in Section 1, $\hat{\mathbf{p}}$ is the dipole moment unit vector. The dyadic Green function of the system is represented by $\overset{\leftrightarrow}{\mathbf{G}} = \overset{\leftrightarrow}{\mathbf{G}}^0 + \overset{\leftrightarrow}{\mathbf{G}}^R$, where $\overset{\leftrightarrow}{\mathbf{G}}^0$ denotes the dyadic Green function for an isolated emitter and $\overset{\leftrightarrow}{\mathbf{G}}^R$ accounts for the contribution of the plasmonic environment. By using the following relations:[9] $\hat{\mathbf{p}} \cdot \mathrm{Im}\{\overset{\leftrightarrow}{\mathbf{G}}^0(\mathbf{r}',\mathbf{r}')\} \cdot \hat{\mathbf{p}} = k'/(6\pi)$ and $\mathbf{E}^R(\mathbf{r}') = \omega^2 \mu_0 \overset{\leftrightarrow}{\mathbf{G}}^R(\mathbf{r}',\mathbf{r}') \cdot \mathbf{p}$, (110) may be rewritten as

$$
\frac{\Gamma}{\Gamma_0} = \frac{P}{P_0} = \sqrt{\varepsilon'}\left[1 + \frac{6\pi\varepsilon_0 \varepsilon'}{(k')^3 |\mathbf{p}|} \hat{\mathbf{p}} \cdot \mathrm{Im}\left\{ \mathbf{E}^R(\mathbf{r}') \right\} \right].
\tag{111}
$$

In (111), for an emitter located outside the studied nanoparticles, $\mathbf{E}^R = \mathbf{E}^S$, see (3); for an emitter located inside the dielectric shell or core, $\mathbf{E}^R = \mathbf{E}^D$, see (8) and (62), respectively.[2,4] Since $\mathbf{E}^R$ is directly proportional to the dipole moment, Γ/Γ_0 is independent of the same parameter.[9,10]

By integrating the normal component of the Poynting vector over the surface of a large sphere, incorporating the emitter and nanoparticle,[1,11] the following expressions are obtained for Γ_{rad}/Γ_0 for an emitter positioned outside and inside the studied topologies, respectively

$$\frac{\Gamma_{rad}}{\Gamma_0} = \frac{P_{rad}}{P_0} = \frac{6\pi\varepsilon_0^2}{k_0^6\sqrt{\varepsilon_M}\,|\mathbf{p}|^2}\sum_{n=1}^{\infty}\sum_{m=-n}^{n}\left[\left|d_{Enm}^+ + a_{Enm}^S\right|^2 + \left|d_{Hnm}^+ + a_{Hnm}^S\right|^2\right] \tag{112}$$

$$\frac{\Gamma_{rad}}{\Gamma_0} = \frac{P_{rad}}{P_0} = \frac{6\pi\varepsilon_0^2}{k_0^6\sqrt{\varepsilon_M}\,|\mathbf{p}|^2}\sum_{n=1}^{\infty}\sum_{m=-n}^{n}\left[\left|a_{Enm}^S\right|^2 + \left|a_{Hnm}^S\right|^2\right]. \tag{113}$$

In (112) and (113), a_{Enm}^S and a_{Hnm}^S, and d_{Enm}^+ and d_{Hnm}^+ denote the scattering coefficients and the coefficients of the fields generated by an emitter (see Section 1), respectively. Lastly, the normalized nonradiative decay rate may be calculated by subtracting the contribution of the radiative decay rate from the total one.[12]

The normalized partial LDOS is defined as[9]

$$\frac{\rho}{\rho_0} = \frac{6\pi\varepsilon'\sqrt{\varepsilon'}}{k'}\,\hat{\mathbf{p}}\cdot\mathrm{Im}\left\{\overleftrightarrow{\mathbf{G}}(\mathbf{r}',\mathbf{r}')\right\}\cdot\hat{\mathbf{p}} \tag{114}$$

where $\rho_0 = \omega^2/(\pi^2 c^3)$ is the LDOS of an isolated emitter in vacuum. Similar to the total decay rate, by using the abovementioned relations for $\overleftrightarrow{\mathbf{G}}^0$ and $\overleftrightarrow{\mathbf{G}}^R$, (114) can be rewritten in terms of the electric field as

$$\frac{\rho}{\rho_0} = \varepsilon'\sqrt{\varepsilon'}\left[1 + \frac{6\pi\varepsilon_0\varepsilon'}{(k')^3\,|\mathbf{p}|}\,\hat{\mathbf{p}}\cdot\mathrm{Im}\left\{\mathbf{E}^R(\mathbf{r}')\right\}\right]. \tag{115}$$

Finally, the normalized orientation-averaged LDOS can be calculated using[13]

$$\frac{\overline{\rho}}{\rho_0} = \frac{1}{3}\frac{\rho_r}{\rho_0} + \frac{2}{3}\frac{\rho_t}{\rho_0} \tag{116}$$

where ρ_r/ρ_0 and ρ_t/ρ_0 correspond to the partial LDOS enhancements for radial and tangential emitters, respectively.

3. Impact of radial and tangential emitters

Fig. S1 depicts the radiative and nonradiative decay rates of radial and tangential emitters in the presence of a sodium core–silica shell nanoparticle. Considering the radiative decay rate, the emitters clearly show different behaviors. While the radial emitter displays a resonance that is followed by an antiresonance,[14] the tangential one first experiences an antiresonance and then a resonance,[15] as demonstrated in Fig. S1a. For the nonradiative decay rate, the tangential emitter only introduces a magnitude offset, compared with the other studied emitter, see Fig. S1b.
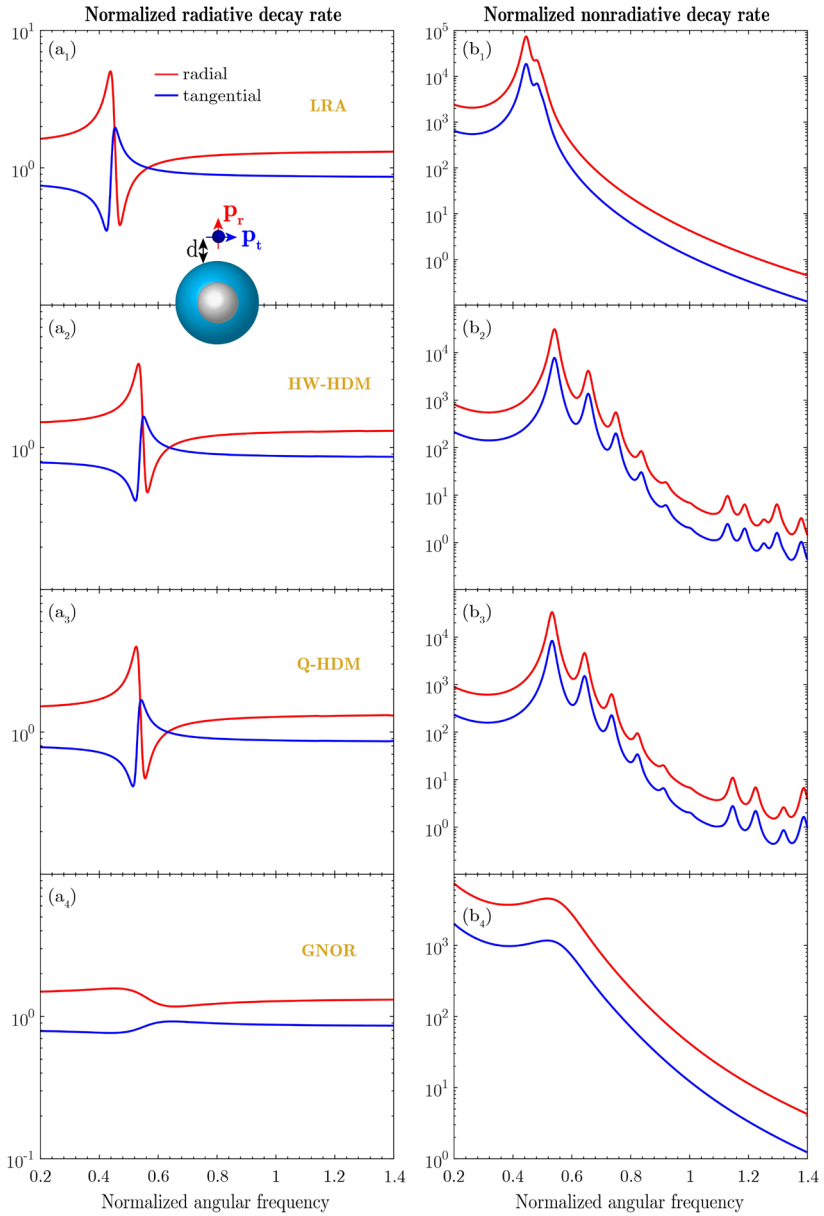
Fig. S1 Response of a sodium core–silica shell nanoparticle with (R_1,R_2) = (1,2) nm and a Drude material parameter, excited by radial and tangential emitters at d = 1 nm. The angular frequency normalized to the plasma frequency is plotted on the horizontal axis. The following features: (a) radiative decay rate and (b) nonradiative decay rate are computed for LRA, HW-HDM, Q-HDM, and GNOR.
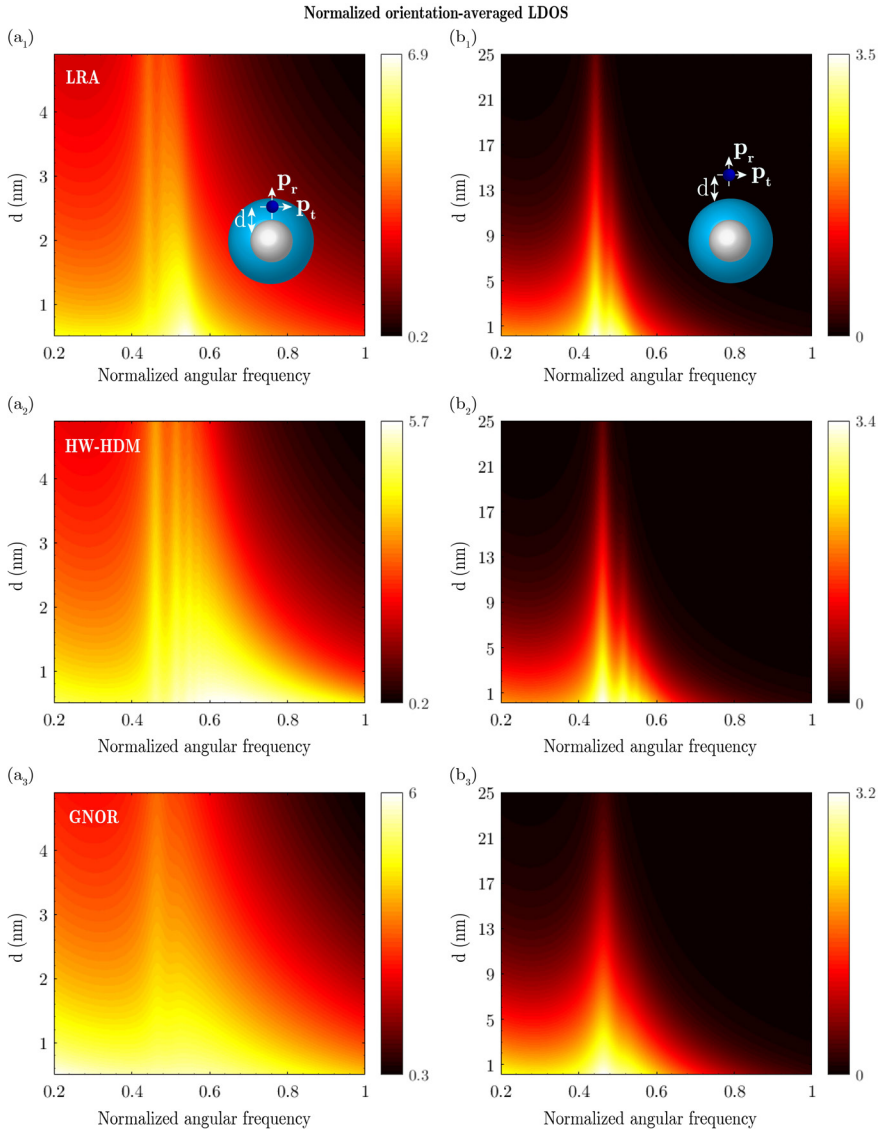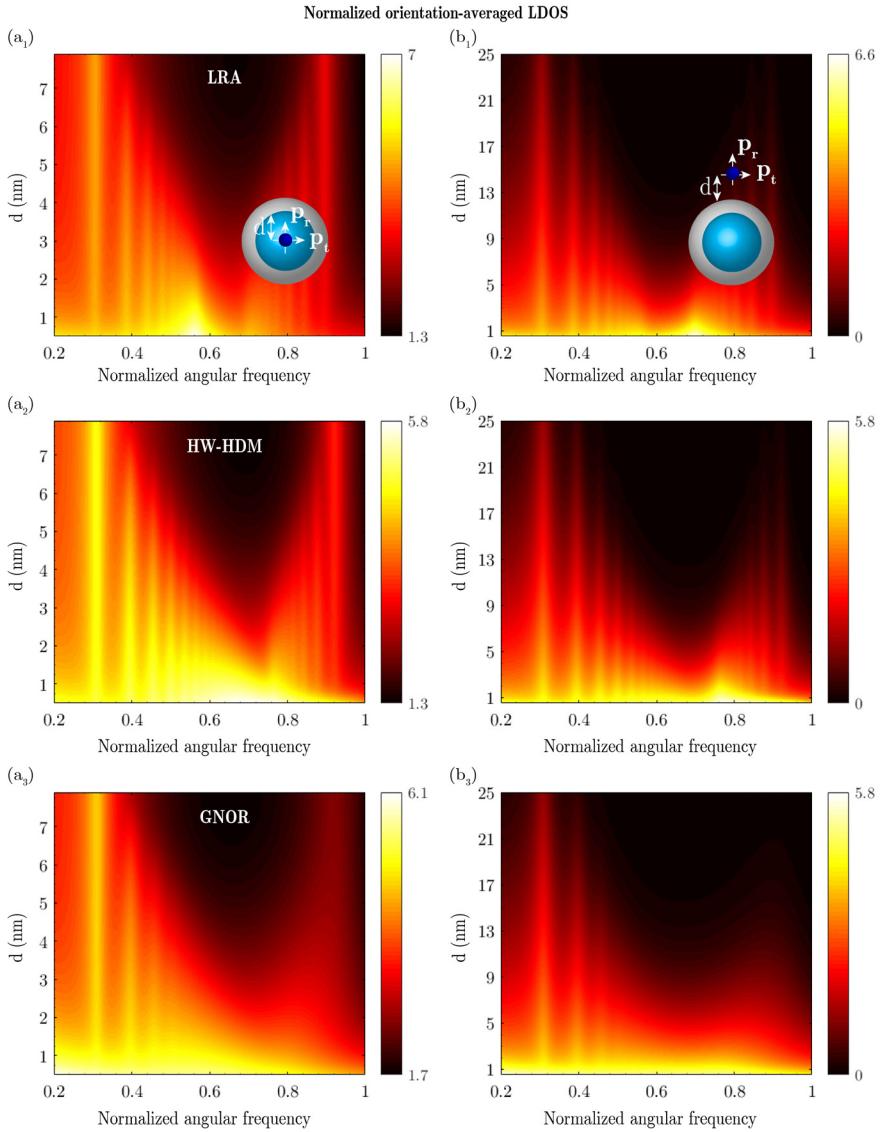
Fig. S2 Response of a sodium core–silica shell nanoparticle with (R_1, R_2) = (5,10) nm and a Drude material parameter. The angular frequency normalized to the plasma frequency is plotted on the horizontal axis. The orientation-averaged LDOS is shown for LRA, HW-HDM, and GNOR, considering an emitter (a) inside and (b) outside the nanoparticle. The results of Q-HDM (not displayed here) are nearly identical to the ones of HW-HDM, for the investigated topology. A $\log_{10}$ scale is used to represent the magnitude of the studied feature.
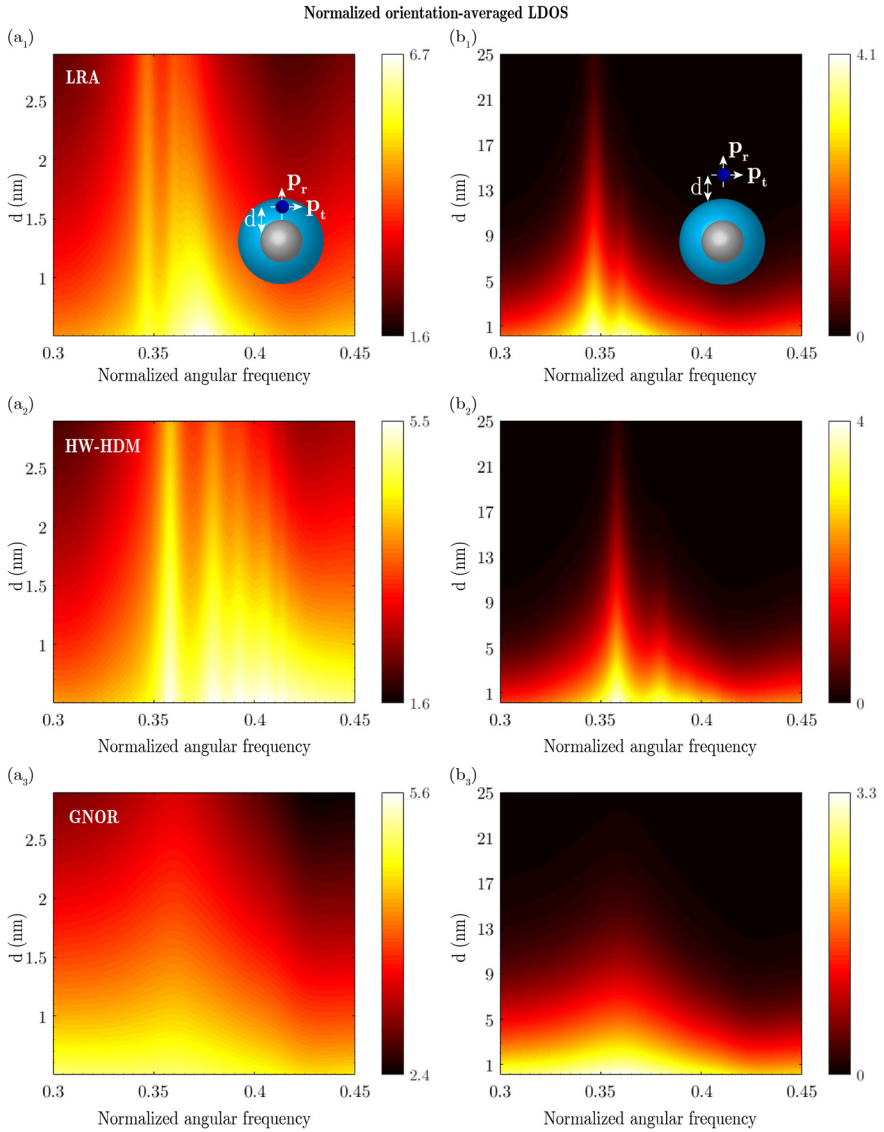
Fig. S3 Response of a silica core–sodium shell nanoparticle with (R_1,R_2) = (8,10) nm and a Drude material parameter. The angular frequency normalized to the plasma frequency is plotted on the horizontal axis. The orientation-averaged LDOS is shown for LRA, HW-HDM, and GNOR, considering an emitter (a) inside and (b) outside the nanoparticle. The results of Q-HDM (not displayed here) are nearly identical to the ones of HW-HDM, for the investigated topology. A $\log_{10}$ scale is used to represent the magnitude of the studied feature.
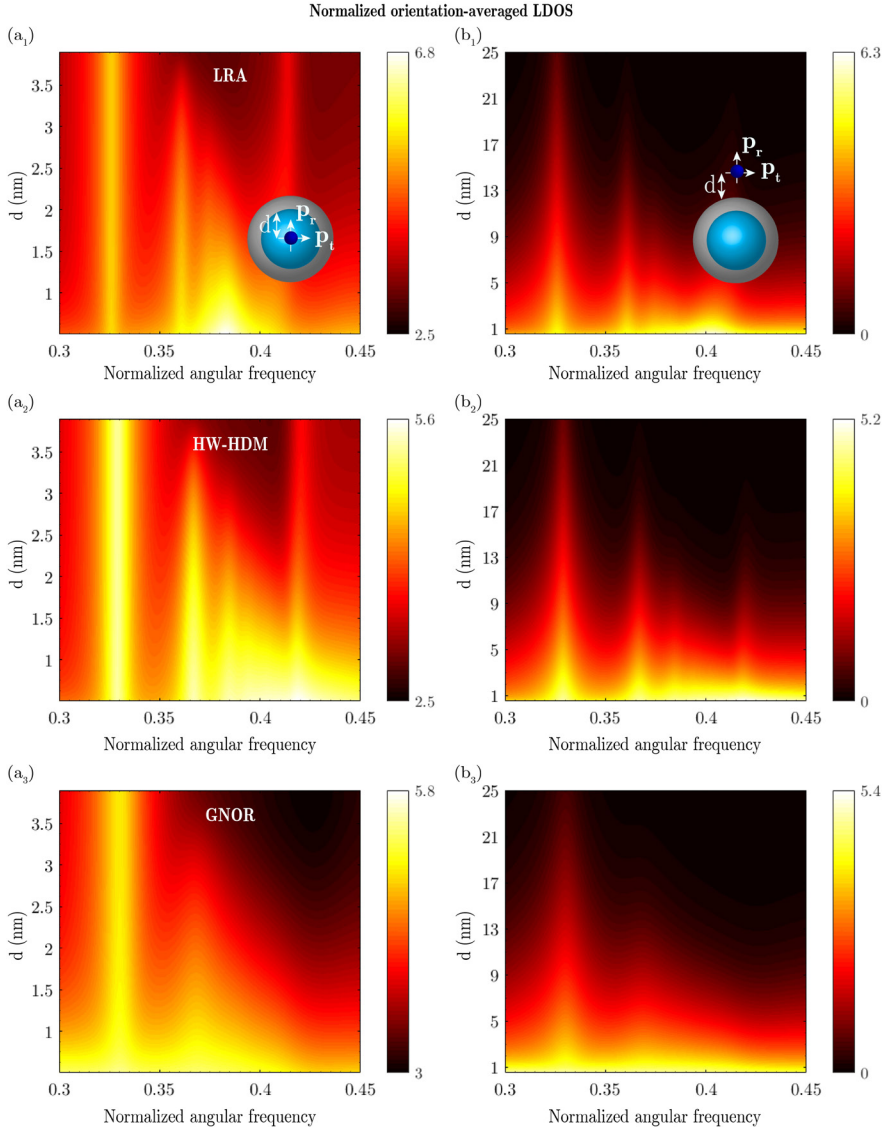
Fig. S4 Response of a silver core–silica shell nanoparticle with $(R_1, R_2) = (3, 6)$ nm and an experimental material parameter. The angular frequency normalized to the plasma frequency is plotted on the horizontal axis. The orientation-averaged LDOS is shown for LRA, HW-HDM, and GNOR, considering an emitter (a) inside and (b) outside the nanoparticle. The results of Q-HDM (not displayed here) are nearly identical to the ones of HW-HDM, for the investigated topology. A $\log_{10}$ scale is used to represent the magnitude of the studied feature.
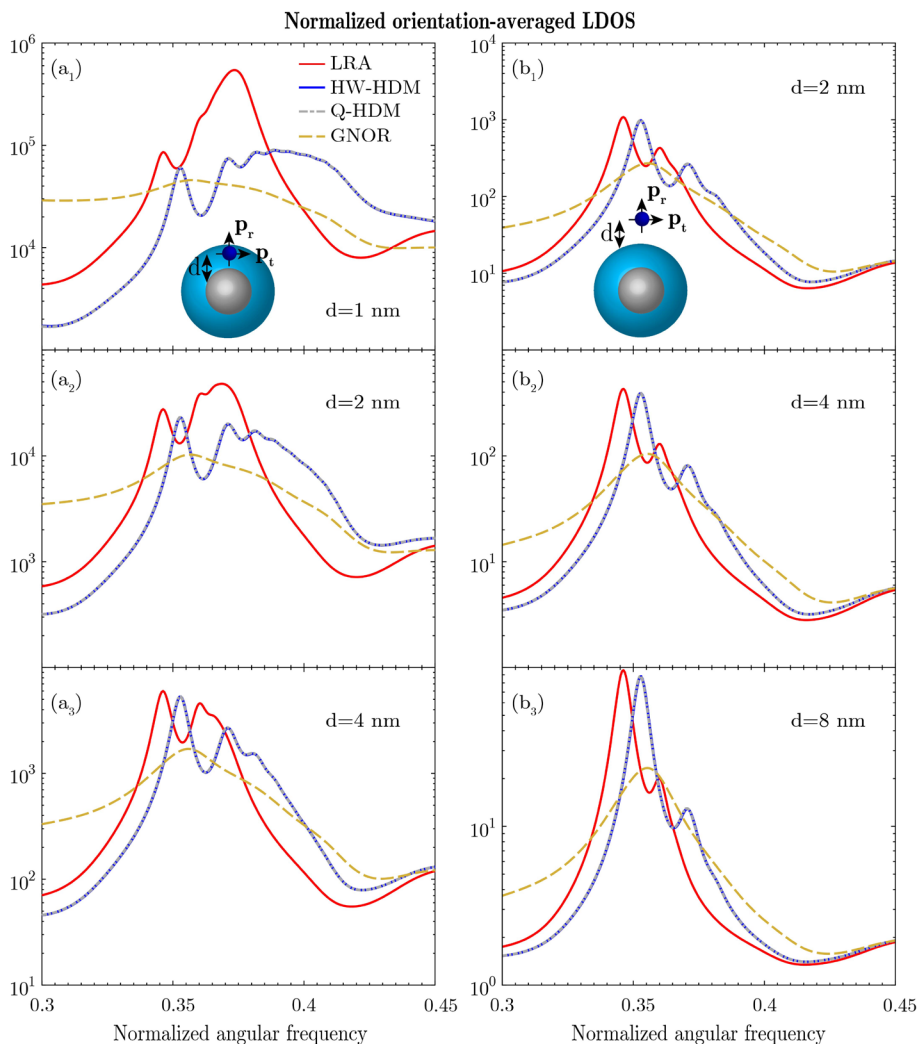
Fig. S5 Response of a silica core–silver shell nanoparticle with (R_1,R_2) = (4,6) nm and an experimental material parameter. The angular frequency normalized to the plasma frequency is plotted on the horizontal axis. The orientation-averaged LDOS is shown for LRA, HW-HDM, and GNOR, considering an emitter (a) inside and (b) outside the nanoparticle. The results of Q-HDM (not displayed here) are nearly identical to the ones of HW-HDM, for the investigated topology. A $\log_{10}$ scale is used to represent the magnitude of the studied feature.

Fig. S6 Response of a silver core–silica shell nanoparticle with $(R_1, R_2) = (5,10)$ nm and an experimental material parameter. The angular frequency normalized to the plasma frequency is plotted on the horizontal axis. The orientation-averaged LDOS is computed for LRA, HW-HDM, Q-HDM, and GNOR, considering an emitter (a) inside and (b) outside the nanoparticle.
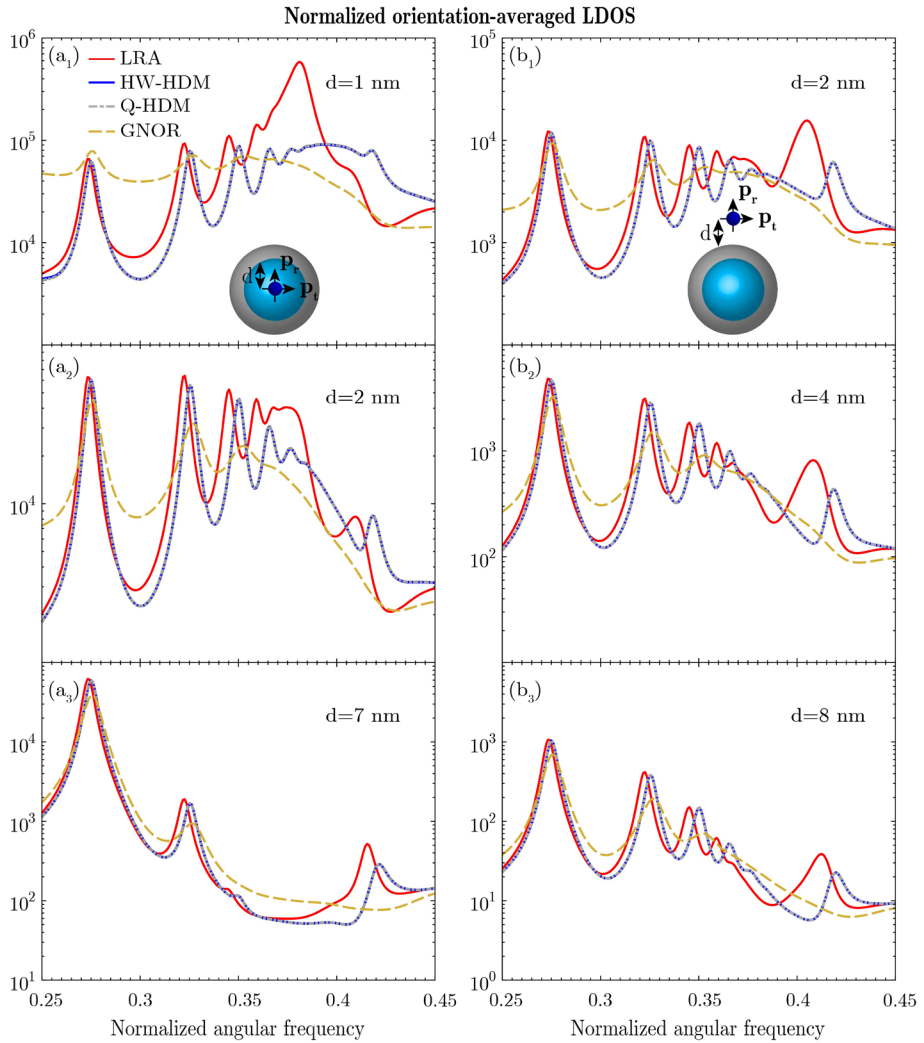
Fig. S7 Response of a silica core–silver shell nanoparticle with $(R_1, R_2) = (8,10)$ nm and an experimental material parameter. The angular frequency normalized to the plasma frequency is plotted on the horizontal axis. The orientation-averaged LDOS is computed for LRA, HW-HDM, Q-HDM, and GNOR, considering an emitter (a) inside and (b) outside the nanoparticle.
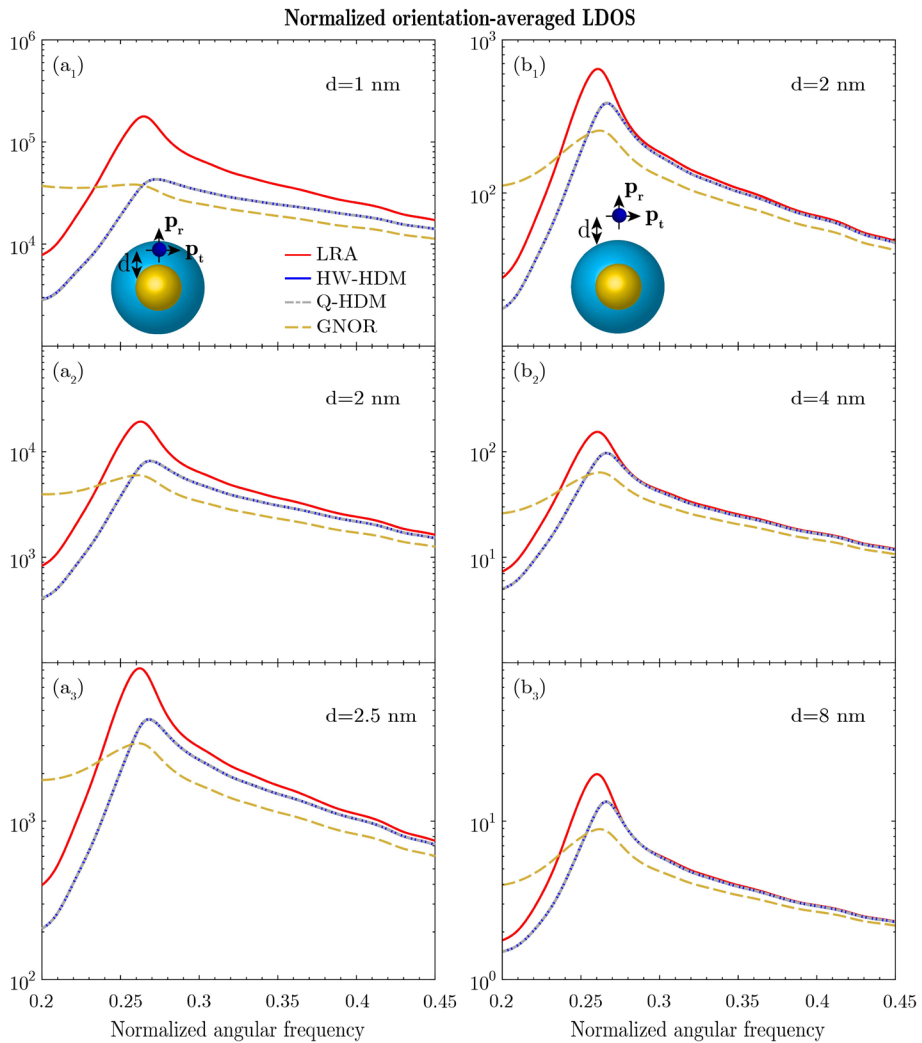
Fig. S8 Response of a gold core–silica shell nanoparticle with $(R_1, R_2) = (3,6)$ nm and an experimental material parameter. The angular frequency normalized to the plasma frequency is plotted on the horizontal axis. The orientation-averaged LDOS is computed for LRA, HW-HDM, Q-HDM, and GNOR, considering an emitter (a) inside and (b) outside the nanoparticle.
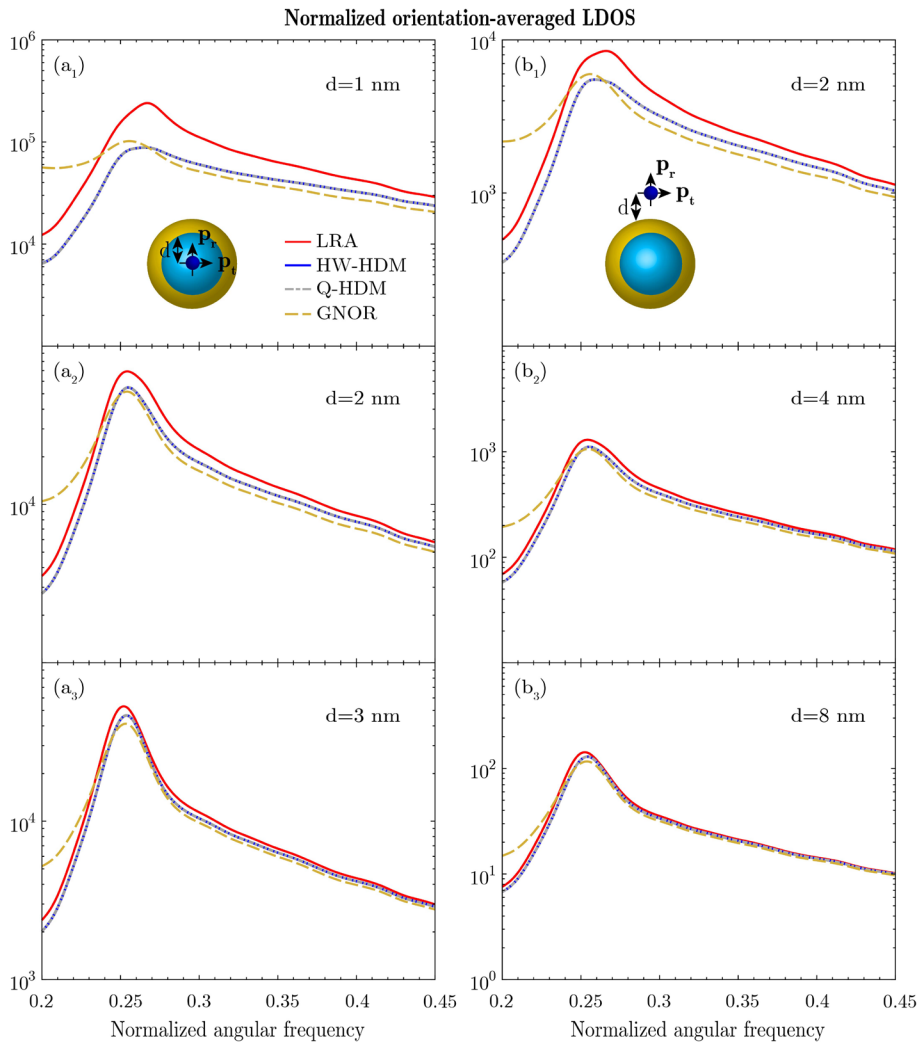
Fig. S9 Response of a silica core–gold shell nanoparticle with (R_1,R_2) = (4,6) nm and an experimental material parameter. The angular frequency normalized to the plasma frequency is plotted on the horizontal axis. The orientation-averaged LDOS is computed for LRA, HW-HDM, Q-HDM, and GNOR, considering an emitter (a) inside and (b) outside the nanoparticle.

References

1   C. Tserkezis, N. Stefanou, M. Wubs and N. A. Mortensen, *Nanoscale*, 2016, **8**, 17532–17541.
2   J. D. Jackson, *Wiley*, Hoboken, USA, 1999.
3   A. Moroz, *Ann. Phys.*, 2005, **315**, 352–418.
4   S. Raza, S. I. Bozhevolnyi, M. Wubs and N. A. Mortensen, *J. Phys.: Condens. Matter*, 2015, **27**, 183204.
5   N. A. Mortensen, S. Raza, M. Wubs, T. Søndergaard and S. I. Bozhevolnyi, *Nat. Commun*., 2014, **5**, 3809.
6   C. F. Bohren and D. R. Huffman, *WILEY-VCH Verlag GmbH & Co. KGaA*, Weinheim, Germany, 2004.
7   M. Kupresak, X. Zheng, G. A. E. Vandenbosch and V. V. Moshchalkov, *Adv. Theory Simul*., 2018, **1**, 1800076.
8   A. Moradi, *Phys. Plasmas*, 2015, **22**, 022119.
9   L. Novotny and B. Hecht, *Cambridge University Press*, Cambridge, UK, 2015.
10 A. E. Krasnok, A. P. Slobozhanyuk, C. R. Simovski, S. A. Tretyakov, A. N. Poddubny, A. E. Miroshnichenko, Y. S. Kivshar and P. A. Belov, *Sci. Rep*., 2015, **5**, 12956.
11 C. G. Khoury, S. J. Norton and T. Vo-Dinh, *Nanotechnology*, 2010, **21**, 315203.
12 H. Y. Chung, P. T. Leung and D. P. Tsai, *J. Chem. Phys.*, 2012, **136**, 184106.
13 T. Christensen, W. Yan, S. Raza, A.-P. Jauho, N. A. Mortensen and M. Wubs, *ACS Nano*, 2014, **8**, 1745–1758.
14 C. Ciracì, R. Jurga, M. Khalid and F. Della Sala, *Nanophotonics*, 2019, **8**, 1821–1833.
15 H. Mertens, A. F. Koenderink and A. Polman, *Phys. Rev. B*, 2007, **76**, 115123.